

Review

Refining Principles and Technical Methodologies to Produce Ultra-Pure Magnesium for High-Tech Applications

Seifeldin R. Mohamed[†], Semiramis Friedrich^{*,†}  and Bernd Friedrich 

IME Institute of Process Metallurgy and Metal Recycling, RWTH Aachen University, 52056 Aachen, Germany; sraslan@ime-aachen.de (S.R.M.); bfriedrich@ime-aachen.de (B.F.)

* Correspondence: SFriedrich@ime-aachen.de; Tel.: +49-241-80-95977

† These authors contributed equally to this work.

Received: 23 November 2018; Accepted: 10 January 2019; Published: 15 January 2019



Abstract: During the last decade, magnesium-based medical implants have become the focal point of a large number of scientific studies due to their perceived favorable properties. Implants manufactured from magnesium alloys are not only biocompatible and biodegradable, but they are also the answer to problems associated with other materials like stress shielding (Ti alloys) and low mechanical stability (polymers). Magnesium has also been a metal of interest in another field. By offering superior technical and economic features in comparison to lithium, it has received significant attention in recent years as a potential battery anode alternative. Natural abundancy, low cost, environmental friendliness, large volumetric capacity, and enhanced operational safety are among the reasons that magnesium anodes are the next breakthrough in battery development. Unfortunately, commercial production of such implants and primary and secondary cells has been hindered due to magnesium's low corrosion resistance. Corrosion investigations have shown that this inferior quality is a direct result of the presence of certain impurities in metallic magnesium such as iron, copper, cobalt, and nickel, even at the lowest levels of concentration. Magnesium's sensitivity to corrosion is an obstacle for its usage not only in biomedical implants and batteries, but also in the automotive/aerospace industries. Therefore, investigations focusing on magnesium refinement with the goal of producing high and ultra-high purity magnesium suitable for such demanding applications are imperative. In this paper, vacuum distillation fundamentals and techniques are thoroughly reviewed as the main refining principles for magnesium.

Keywords: magnesium; refining; recycling; ultra-high purity; vacuum distillation; condensation

1. Introduction

In today's high-tech, application-oriented world, the demand for materials with superior quality suiting these applications is on the rise. Moreover, such materials should also be resource-saving and environmentally friendly. That is the reason for the recent significantly growing attention to magnesium, the lightest of the structural metals. Magnesium's extremely low density in comparison to iron and even aluminum results in lower energy consumption, which has made it attractive for automotive and aerospace industries in the last few decades. Not only this, but its high thermal and electrical conductivity, high alkaline resistivity, dimensional stability in electronic housing, as well as the machinability and formability of magnesium also make it a favorable metal for various applications [1,2].

Typically, magnesium is found in the Earth's crust in the form of dolomite ($\text{CaCO}_3 \cdot \text{MgCO}_3$), magnesite (MgCO_3), and magnesium oxide (MgO), among others. Regarding liquid resources,

magnesium is usually found in form of carnallite ($\text{KCl}\cdot\text{MgCl}_2\cdot 6\text{H}_2\text{O}$) and bischofite ($\text{MgCl}_2\cdot 6\text{H}_2\text{O}$) [3]. For primary magnesium production there are two routes: electrolytic or thermal processing. USA, Canada, and some EU countries have dominated magnesium production from the 1970s to the 1990s, using electrolytic methods such as the Dow process. However, since the start of the 21st century, the growth in Chinese magnesium production capacity has led to the almost complete decline of western magnesium and the electrolytic route. China's adoption of the Pidgeon process (thermal route) enabled it to be the world's biggest producer, due to the relative easiness, versatility, and reduced capital cost of this process. Despite these great advantages, the Pidgeon process consumes a significant amount of energy, requires high labor costs, and suffers from low productivity (a batch process): aspects that make this process unfeasible to utilize in any other country [4]. The Pidgeon and the Dow processes are not the only examples of their respective processing routes. Processes like Magnetherm and Mintek have also emerged over the years as substitutes for the Pidgeon process.

It should be noted that all of these processes are primary processes to extract magnesium from its various ores and are not appropriate for extreme refining/purification purposes, as they are only capable of producing metallurgical grade pure Mg. Typically, electrolytic processes can produce Mg with 99.8% purity [4]. Even to this day, US Magnesium LLC (one of the few remaining magnesium producers using the electrolytic route) offers its pure magnesium in this grade. Regarding thermal processes, they can also produce comparable Mg purities; 99.97%, 99.93%, and 99.02% by the Pidgeon, Magnetherm, and Mintek processes respectively, with these figures obtained by considering only the main impurities (Al, Si, Ca, and Fe) [4,5]. The magnesium produced by such processes is classified as 'pure' by the ASTM, as they use this term for Mg with purities between 99.8% and 99.98% (3N) [6]. This level of purity is typically enough when talking about most conventional industrial applications of magnesium, as shown with their consumption rates in Figure 1 [7].

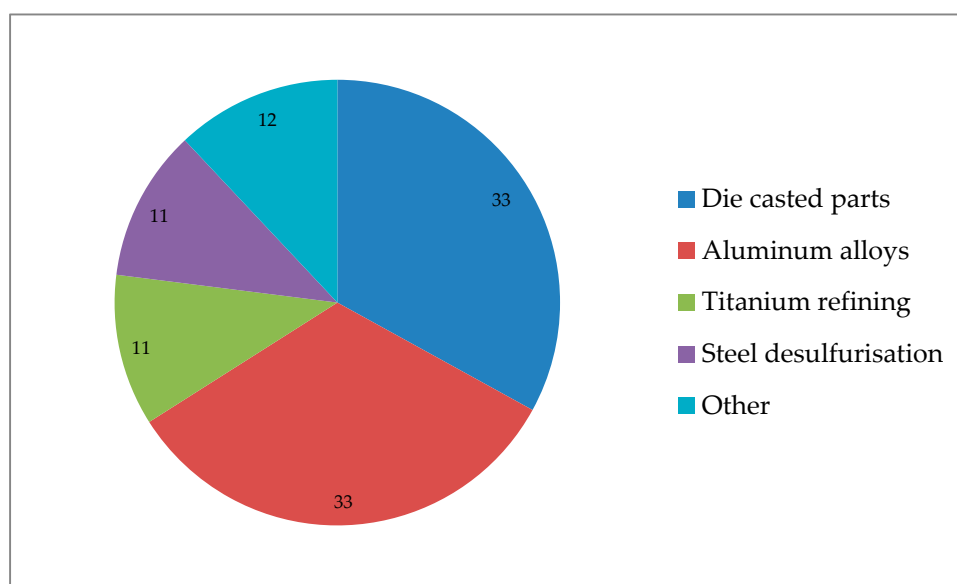


Figure 1. Global consumption of major Mg applications in 2012 (in %).

However, a quite trendy application of magnesium is Mg-based implants, which has recently become one of the most researched areas in the world of magnesium, and for which the commercial purity grade is not sufficient. For almost a decade, magnesium alloys were and still are under extensive investigation to test their feasibility as a superior replacement for titanium alloys and polymer-based implants. Magnesium alloys solve the problems associated with the other materials like stress shielding and mechanical stability for titanium and polymer based implants respectively [8,9]. Moreover, magnesium has antibacterial properties, is biocompatible and biodegradable, and eliminates the need for further surgical intervention to remove the implant after healing [10–12].

Last but not least, another trendy application of magnesium in recent years is magnesium-based anodes in batteries. Since magnesium is an abundant, light, environmentally friendly metal and it is significantly cheaper than lithium, it is a highly feasible alternative for lithium. Additionally, it eliminates the toxic effects related to discarding or recycling of lithium batteries [13]. Moreover, magnesium possesses almost double the volumetric energy density of lithium, and offers improved operational safety due to the lack of non-dendritic deposition and lower air sensitivity [14].

For these sorts of high-tech applications, magnesium purity must be upgraded to high (4N) and ultra-high (5N or more) purity graded Mg [15,16], because their development is hindered by the weak corrosion resistance of magnesium. Extensive research has found that magnesium corrosion is extremely sensitive to impurity elements such as iron, nickel, copper, and cobalt at even ppm levels, as illustrated in Figure 2 [17]. These impurities generally tend to be highly cathodic in a Mg matrix, thus forming micro-galvanic cells that result in severe corrosion [18]. In the case of biomedical applications, this corrosion behavior compromises the mechanical integrity of the implant and shortens its estimated service life [19]. An optimum corrosion rate accompanied by a symmetric laminar degradation can be achieved by using high purity magnesium [20]. Even after achieving tolerable levels of the above mentioned hazardous impurity elements to control corrosion, their toxic effect is another matter that drastically decreases the permissible limit [21]. When it comes to batteries, the corrosion of the anode is undesired as it results in the formation of a passive layer that blocks the electrode, which leads to a decrease in efficiency and unstable anodic dissolution, as well as a decrease in the output voltage [22].

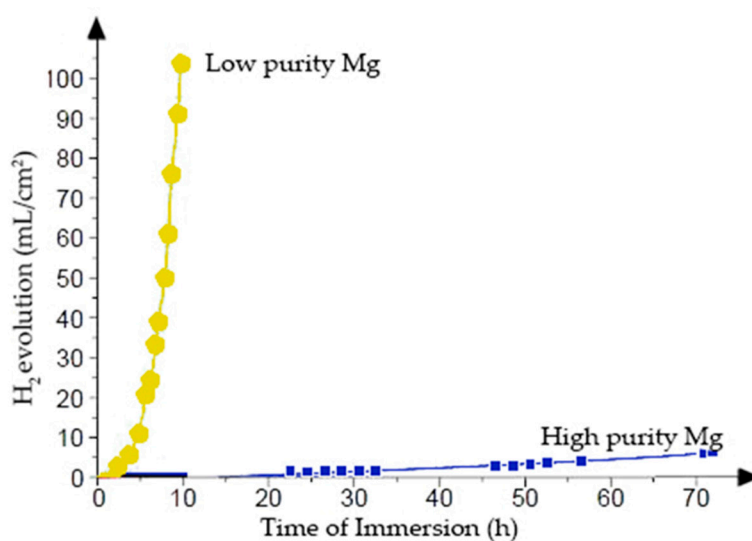


Figure 2. High purity Mg vs. low purity Mg corrosion rates.

The focus of this paper is to introduce the most important magnesium refining processes used to achieve high and ultra-high purity magnesium, with the aim of giving an extensive overview on the principles and the devised techniques and setups. Various methodologies have been investigated over the years to test their feasibility in producing ultra-high purity 'XHP' magnesium, such as electro-refining by using fluorides, chlorides, or oxides as the electrolytes. Impurity precipitation was also investigated as a potential methodology for this task. Electro-refining was distinguished to be a complex trial with high energy consumption and large operation costs, while impurity precipitation has not been successful in effectively and economically producing XHP magnesium. Therefore, vacuum distillation is still the only reliable and cost-effective process for this purpose [15,23]. Before introducing different methodologies based on vacuum distillation, the fundamentals of this principle will be briefly explained in the following section.

2. Fundamentals of Vacuum Distillation

Vacuum distillation offers several advantages when it comes to purification of metals. Besides reliable prevention of any contact to atmosphere, dramatic evaporation and sublimation rates at much lower temperatures can be achieved in a vacuum in comparison to the normal atmospheric or inert conditions. This, of course, decreases the reaction time, energy consumption, and operation cost, hence increasing the overall profitability of the process. Furthermore, vacuum distillation is environmentally friendly, as it hinders the formation of exhaust gases, waste water, or slags [24,25].

Distillation in general is based on the fact that different chemical substances (elements or compounds) have different boiling points, hence different vapor pressures. It means that upon heating any given feed material, the more volatile substances evaporate, leaving the less or non-volatile substances in the initial container. It is a fact that each substance has a certain vapor pressure at any given temperature (the only variable), independent of the mass or the volume of that substance [26,27]. In order to represent the vapor pressures of materials depending on their temperature, the following equation is used [28]:

$$\log p^* = AT^{-1} + B \log T + CT + D \quad (1)$$

where p^* is the saturated vapor pressure of pure substances (Pa) and T is the absolute temperature (K). Regarding A , B , C , and D , they are evaporation constants for different elements, for which the exemplary values are shown in Table 1.

Table 1. Values of evaporation constants for Mg and its typical impurities [28].

Element	A	B	C	D	Temperature Range (K)
Ca	−9350	−1.39	0	14.94	298–1112
Cu	−17770	−0.86	0	14.42	298–1356
Fe	−21080	−2.14	0	19.02	298–1809
Mg	−7780	−0.855	0	13.54	298–923
Mg	−7550	−1.41	0	14.915	923–1363
Mn	−14920	−1.96	0	18.32	298–1517
Pb	−10130	−0.985	0	13.28	600–2013
Zn	−6620	−1.255	0	14.465	692–1773

By solving Equation (1) with the evaporation constants mentioned in Table 1, the vapor pressures of these impurities (among others) can be compared to that of Mg. Preliminary results indicate the feasibility of the distillation process, as illustrated in Figure 3, where all common magnesium impurities except zinc have a lower vapor pressure than magnesium [28]. Therefore, in a magnesium vacuum distillation process, most of the impurities will be expected to stay in the crucible as residue, while Mg and Zn will be collected on a condensing surface.

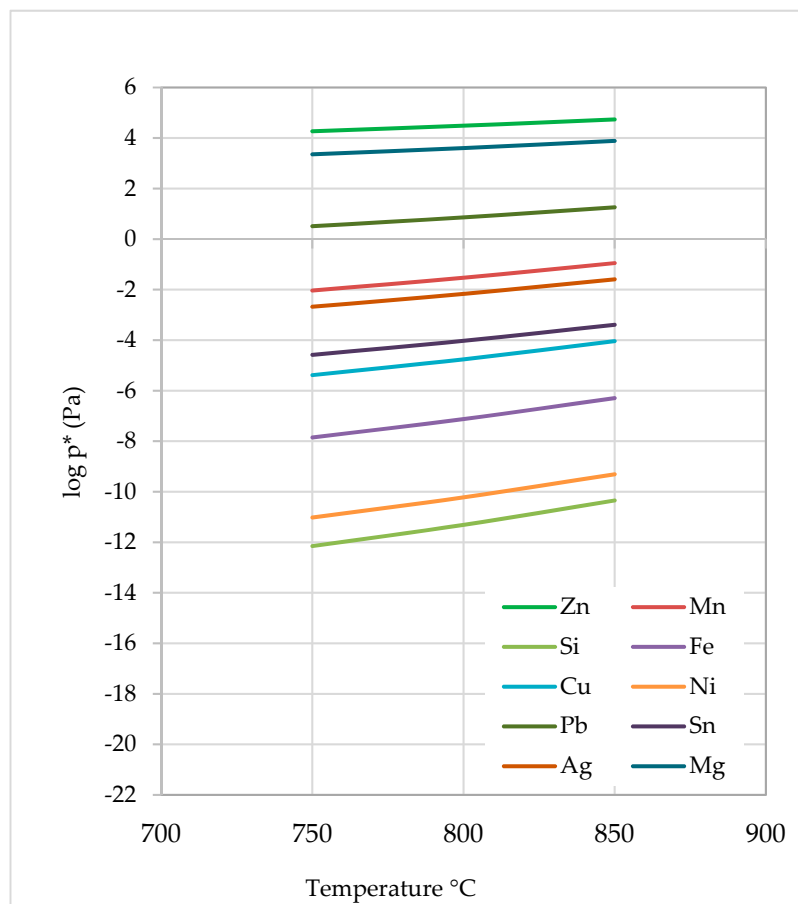


Figure 3. The variation of $\log p^*$ versus temperature for Mg and selected impurities.

It should be noted that the vapor pressure of pure substances is only a preliminary indicator as to the feasibility of the separation process; therefore, a more accurate parameter is devised to show the extent of separation between an impurity element and liquid magnesium. That parameter is the so called separation coefficient (β), which depends on the vapor pressures of both investigated elements as well as their activity coefficients (γ). The separation factor of an exemplary impurity element (i) is to be calculated as shown in Equation (2) [23,29,30].

$$\beta_i = \frac{\gamma_i}{\gamma_{Mg}} \cdot \frac{p_i^*}{p_{Mg}^*} \quad (2)$$

where γ_{Mg} is taken approximately as unity (due to the almost pure raw Mg). Obtaining (γ_i) is the main challenge, because it varies with the temperature of the system and the initial concentration of each impurity. In order to theoretically predict the activity coefficients, the molecular interaction volume model (MIVM) was developed on the basis of statistical thermodynamics [31]. Various studies have used this model to explain the behavior of impurity elements in Pb- and Sn-based alloys during vacuum distillation, reporting comparable results to their experimental trials, hence proving the feasibility of this model for vacuum distillation [32–34].

Another approach to calculate the separation coefficients is the use of an empirical formula Equation (3) to obtain the evaporation coefficient (α_i) [30].

$$y_i = 100 - 100 \left(1 - \frac{x_i}{100}\right)^{\alpha_i} \quad (3)$$

where x_i and y_i are the evaporated wt. % from the main metal and an impurity respectively, calculated from the results of the process. The obtained evaporation coefficient is then substituted into Equation (4) to calculate the separation factor [30].

$$\beta_i = \alpha_i \sqrt{\frac{M_i}{M_{Mg}}} \quad (4)$$

where M_i and M_{Mg} are the molar masses of the investigated impurity and magnesium, respectively. The farther the separation coefficient is from unity, the better the separation between the given impurity and magnesium or vice versa. Table 2 shows the calculated coefficients of some impurities at various temperatures and their (with the exception of zinc) easy separation possibility from magnesium. In this trial-dependent model, the calculated separation coefficient is then used to calculate the activity coefficient of the corresponding impurity through Equation (2).

Table 2. Separation coefficients between Mg and impurities at different temperatures [23].

T (K)	β_{Ca}	β_{Cu}	β_{Pb}	β_{Zn}
873	1.08×10^{-5}	3.98×10^{-12}	4.74×10^{-7}	1.03
923	1.31×10^{-5}	1.66×10^{-11}	6.58×10^{-7}	0.85
973	1.72×10^{-5}	6.58×10^{-11}	9.74×10^{-7}	0.79
1023	2.12×10^{-5}	2.20×10^{-10}	1.34×10^{-6}	0.72

It is worth noting that calculation of the activity coefficients is also important for the prediction of the impurity mass fraction in the gas phase, with the result also depending on the initial concentration of the impurity in the liquid and the vapor pressures of Mg and the investigated impurity [23].

$$i_g = \left[1 + \left(\frac{Mg_l}{i_l} \right) \cdot \left(\frac{\gamma_{Mg}}{\gamma_i} \right) \cdot \left(\frac{p_{Mg}^*}{p_i^*} \right) \right]^{-1} \quad (5)$$

where l and g stand for liquid and gas phases, and Mg_l , i_l , and i_g are the mass fractions of Mg and any given impurity in the liquid and gas phase respectively.

It should be noted that for vacuum distillation, the kinetic aspect is as important as the thermodynamic one, but since the kinetics of this process are highly dependent on the geometry of the used reactor, it is very difficult to obtain information applicable to the process in general, and thus the kinetic aspect will not be discussed in this review.

3. Vacuum Distillation Setups for Producing Ultra-High Purity Magnesium

Vacuum distillation has been investigated as a way to refine magnesium to unprecedented purities throughout the years. In 1978, Revel et al. [35] created a vertical retort (see Figure 4) for magnesium refining. The equipment is composed of a graphite crucible and a diaphragm holding a stainless steel condenser that contains baffles. The system is heated via a resistance heater situated between two sintered alumina walls, with the external wall isolating the equipment.

The design of the system allows a homogeneous temperature at the bottom part (crucible to diaphragm) and a decreasing temperature throughout the condenser's compartments. The apparatus is able to distill a 50 g load of magnesium.

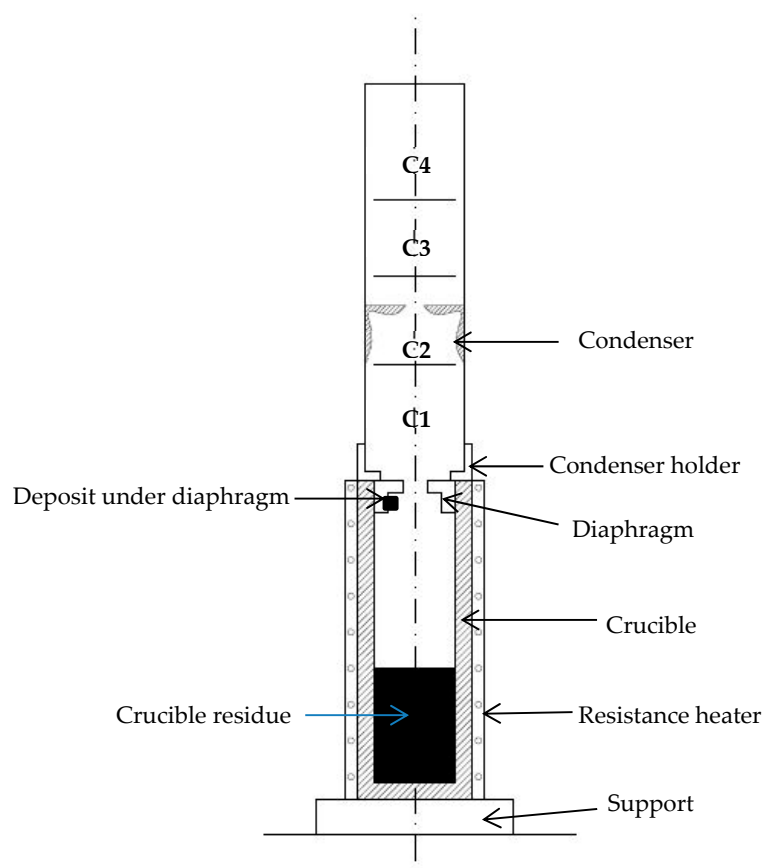


Figure 4. Illustration of Revel's distillation column (C1–C4: compartments of condenser).

The aim of their study was to find the optimum parameters and the effect of various process parameters on the purification degree of impurities with higher volatility than magnesium (e.g. Na, Zn) as well as with low volatility (e.g. Cu, Fe, and Mn). They investigated the effect of the load and condensation temperatures, residual gas pressure, distillation rate, and distilled quantity. The optimum load temperature for this process is 700 °C, and no benefit for increasing the temperature over this value was observed. Regarding the residual gas pressure in the retort, no significant effect on the process was noticed at low pressure levels (0.013 to 0.0013 mbar). The purest deposits of magnesium were found in the lower compartment of the condenser (C1), which had a temperature varying between 400 and 450 °C, having a noticeable difference with deposits condensed below 350 °C. Several distillation rates were investigated (3.5, 24, and 50 g/h) at the optimum temperature by changing the number and size of holes in the diaphragm.

The lowest rate was proven to be the optimum, as it simplifies the control and the reproducibility of the conditions. Table 3 shows a comparison between the impurity concentrations of selected impurities after different stages of distillation. The results shown are of a trial conducted with the mentioned optimum parameters, and the sample is collected from the C1 compartment.

Table 3. Impurity concentration (in ppm) in samples with varying distillation quantity [35].

Element	Before Distillation	After 55% Distillation	After 72% Distillation	After 83% Distillation
Cu	3	0.8	0.6	0.05
Fe	97	<0.07	<0.04	<0.6
Mn	17–19	0.2	0.05	0.01
Na	4.3	0.4	0.3	0.6
Zn	52–58	17	16	17

Despite the extremely high volatility of sodium and zinc, and thus the difficulty to separate them from Mg in a distillation process, the results of Table 3 show a decrease in their concentration. This can be attributed to the multi-chambered condenser, where these elements tend to condense in the upper, low-temperature chambers, while most of the Mg distillate (almost 90%) condenses/solidifies in the lowest chamber [35].

In 1996, Lam and Marx devised a distillation column able to produce Mg with 5N metallic purity [15]. This column (depicted in Figure 5) comprises a crucible and a vertical condenser with multiple baffles, all made out of highly pure graphite. This setup is maintained in a resistance furnace, including three temperature-controlled zones. Through optimization of the baffle positions and temperature control, impurities with higher condensation temperatures than magnesium, such as iron and copper, condense on the lower baffles, while magnesium deposits on the middle ones. Finally, elements such as zinc (as well as sodium and potassium, if present) with lower condensation temperatures condense on the higher positioned baffles. The preferred parameters here are a strong vacuum of 1.3×10^{-6} mbar, a crucible temperature of approximately 700 °C, and condenser temperatures of approximately 600 and 450 °C for the lower and upper parts of the condenser respectively [15].

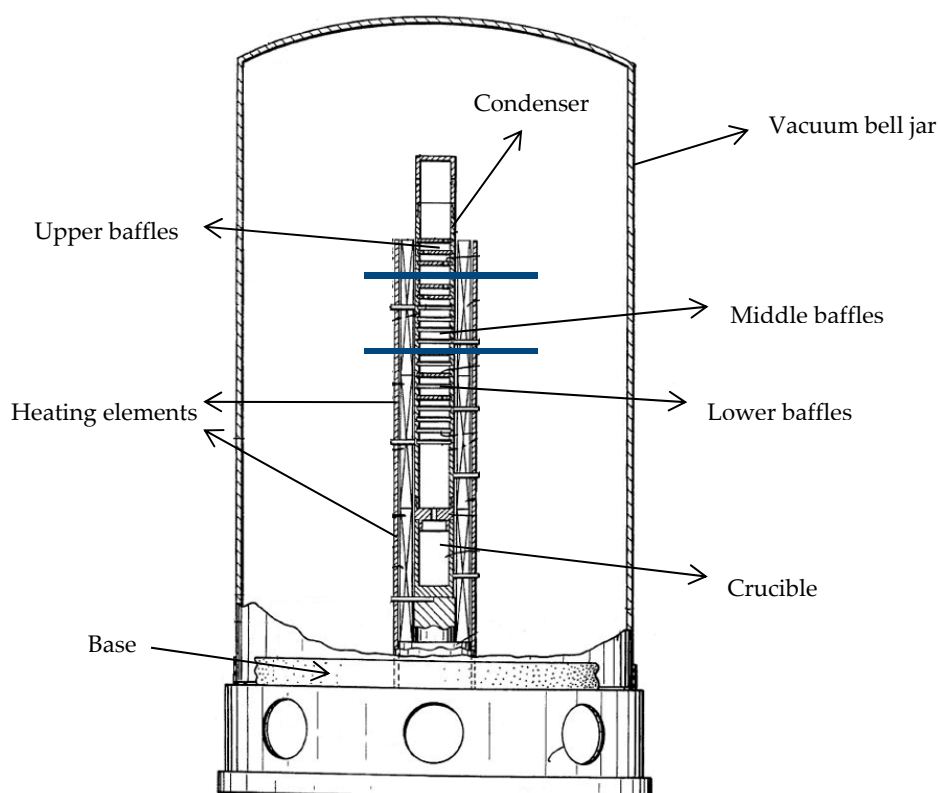


Figure 5. Vacuum distillation column as devised by Lam and Marx.

In 2003, Tayama and Kimura [16] developed a purification method with a newly devised apparatus. Their main concern was to produce XHP magnesium through overcoming some disadvantages they thought present in the Lam and Marx's version of the distillation column. They argued that since the concept of the old apparatus was based on selectively condensing different elements in different temperature zones, it would be difficult to exclude impurities with small differences in solidification temperatures between them and magnesium, especially on an industrial scale. Of course, in order to ensure the exclusion of such elements, the specified recovery zone must have a very small temperature range, which will result in a low metal yield.

This apparatus is also a vertical distillation column, comprising a feed heating zone at the bottom and a condensation/passage way zone thereupon. A cooled chamber is then located above for the condensation and collection of the purified magnesium. At the top, there is an entrapment zone to collect any vapor that is still not solidified. As shown in Figure 6 [16], there are special vapor passage plates, some downwardly convex plates with a centered hole, and some upwardly convex plates with peripheral holes.

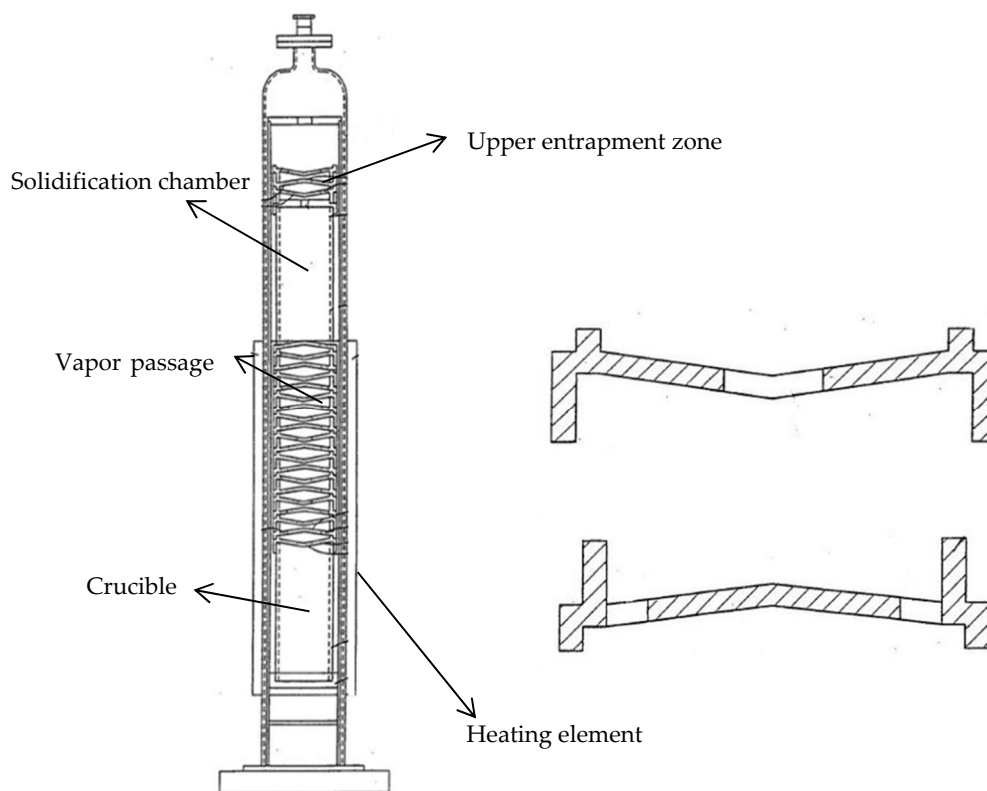


Figure 6. Vacuum distillation column as devised by Tayama and Kimura (left) and vapor passage plates (right).

The intention of these types of plates is to force the generated magnesium vapor to follow a zigzag path that sufficiently decreases its flow rate. The continuous collisions between the vapor and the plates result in energy losses, thus decreasing the vapor temperature and allowing part of the evaporated Mg to condense on the vapor passage plates. The design and the installation order of these plates allow magnesium vapor to pass upwardly, and at the same time allow the condensed melt (that still contains some impurities) to flow downwards until it eventually reaches the feed crucible. Through this countercurrent mechanism, fractionation of high vapor pressure elements (i.e., magnesium) and low vapor pressure elements (i.e., impurities except zinc) occurs. The Mg vapor escaping the passage then solidifies on the walls of the solidification chamber, while the remaining fumes (Zn–Mg mixture) are collected by the upper entrapment zone of the reactor. The optimum parameters reported were a vacuum atmosphere of 1.3×10^{-3} mbar along with controlled temperatures of 750 °C and 700 °C for the feed crucible and the condensation vapor passage plates respectively. Magnesium with an impurity content of 0.75 ppm (6N purity) can be obtained. If the obtained material from the first run is purified again through the same process, this impurity level is able to be reduced to 0.38 ppm (6N6). It should be noted that these values exclude zinc, as the amount of zinc in the final material after two runs is still 1.7 ppm, which increases the total impurity content to 2.08 ppm, resulting in Mg with 5N8 purity grade being produced [16].

In all the above setups, the condensed magnesium is always collected as fine powdery crystals with high surface/volume ratio. Due to the extremely high reactivity of magnesium, these fine particles can be easily oxidized, leading to problems upon re-melting to produce a semi-finished product, because the formed oxide skins on the fine crystals contaminate the pure melt and remain in the solidified metal in the form of non-metallic inclusions. This, of course, can have severe consequences not only on the mechanical properties of the finished product, but also on its corrosion resistance. In order to overcome this problem, Uggowitz et al. [36] developed a quite different setup (see Figure 7) that allows the liquid condensation of pure magnesium, so that upon solidification it is collected as a considerable amount of bulk. In this setup, magnesium is heated in a resistance-heated stainless steel retort until evaporation. Since the produced vapor reacts weakly with the stainless steel of the walls, minor contamination can be detected in the condensed molten magnesium droplets. In order to prevent these contaminated droplets from entering the collection crucible, a 'cover' is placed to direct the falling droplets back into the feed. By controlling and keeping the temperature constant via an independent heating element, under the boiling point but over the melting temperature of magnesium, the evaporated magnesium that enters the collection crucible is to be condensed in a liquid state [36].

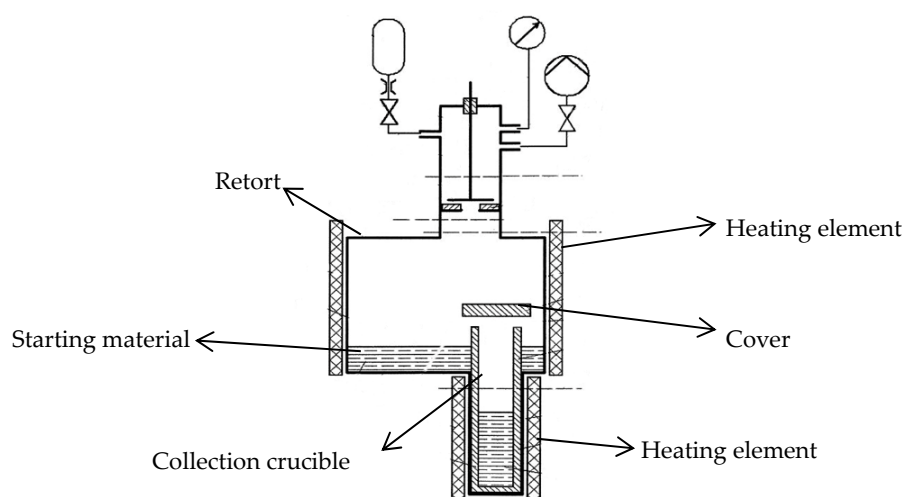


Figure 7. Vacuum distillation retort as devised by Uggowitz et al.

4. Summary and Outlook

In the never ending search for better materials and technologies to reduce production—as well as environmental—costs, researchers have given special attention to magnesium in previous years for its exceptional qualities. This has led to a significant rise in the production of magnesium, to meet the increasing demand. The major reason hindering the extensive use of magnesium (i.e., weak corrosion resistance) comes from the presence of impurities like iron, cobalt, copper, and nickel, even at minor quantities. To overcome this issue and unlock magnesium's full potential as a biodegradable metal and a battery anode, various methodologies for ultra-purification of magnesium have been investigated over the years.

Throughout this paper, the major refining process for magnesium (i.e., vacuum distillation) was deeply reviewed, discussing the refining principle and the most important setups devised over the years, especially the ones focusing on ultra-purification. The review shows that magnesium with purities up to 5N8 can be achieved by vacuum distillation, with zinc being the main reason for not achieving purity values over 6N.

Despite the efforts of the past years, there is still a big gap in the thermodynamic data. Except for the limited information mentioned in Section 2, no data for the activity coefficients or the separation factors of impurities in magnesium are available. A MVIM study to theoretically predict the behavior

of such impurities and confirm the results with experimental trials would drastically enhance our understanding for the process. An extensive kinetic study showing the effect of the evaporation rate on the purification levels of the various impurities is also an interesting topic for further research. For elements difficult to separate from Mg (e.g., zinc), investigating the addition of certain elements to the melt to form a hardly evaporable intermetallic compound could also be a feasible technique. Finally, in an effort to find further successful magnesium refining techniques, the authors are keen on testing the feasibility of fractional crystallization-based methods too.

Author Contributions: B.F. was the principal investigator. S.R.M. and S.F. wrote and edited the manuscript.

Funding: This research received no external funding.

Conflicts of Interest: The authors declare no conflict of interest.

References

1. Avedesian, M.M.; Baker, H. Magnesium and Magnesium Alloys. In *ASM Speciality Handbook*; ASM International: Materials Park, OH, USA, 1999.
2. Engh, T.A. *Principles of Metal Refining*; Oxford University Press: Oxford, UK, 1992; ISBN 9780198563372.
3. Pekguleryuz, M.; Kainer, K.; Kaya, A. (Eds.) *Fundamentals of Magnesium Alloy Metallurgy*; Elsevier: New York, NY, USA, 2013.
4. Wulandari, W.; Brooks, G.; Rhamdhani, M.; Monaghan, B. Magnesium: Current and Alternative Production Routes. In *Australian Conference on Chemical Engineering*; University of Wollongong Australia: Wollongong, Australia, 2010.
5. Pekguleryuz, M.; Mackenzie, L. (Eds.) Pilot Plant Demonstration of the Mintek Thermal Magnesium Process. In *Proceedings of the Conference of Metallurgists, Montréal, QC, Canada, 1–4 October 2006*.
6. Charles, M. (Ed.) *Engineering Properties of Magnesium Alloys*; ASM International: Novelt, OH, USA, 2017.
7. Magnesium.com. Dynamics of Worldwide Magnesium Metal Consumption, 2008–2013. Available online: <http://www.magnesium.com/w3/data-bank/index.php?mgw=241> (accessed on 15 September 2018).
8. Beevers, D.J. Metal vs. bioabsorbable interference screws: Initial fixation. *Proc. Inst. Mech. Eng. Part H J. Eng. Med.* **2003**, *217*, 59–75. [[CrossRef](#)]
9. Breen, D.J.; Stoker, D.J. Titanium lines: A manifestation of metallosis and tissue response to titanium alloy megaprotheses at the knee. *Clin. Radiol.* **1992**, *47*, 274–277. [[CrossRef](#)]
10. Witte, F.; Hort, N.; Feyerabend, F. Degradable biomaterials based on magnesium corrosion. *Curr. Opin. Solid State Mater. Sci.* **2008**, *12*, 63–72. [[CrossRef](#)]
11. Staigera, M.P.; Pietaka, A.M.; Huadmaia, J.; Dias, G. Magnesium and its alloys as orthopedic biomaterials: A review. *Biomaterials* **2006**, *27*, 1728–1734. [[CrossRef](#)] [[PubMed](#)]
12. Hort, N.; Huangand, Y.; Feyerabend, F. Magnesium alloys as implant materials—Principles of property design for Mg–RE alloys. *Acta Biomater.* **2010**, *6*, 1714–1725. [[CrossRef](#)] [[PubMed](#)]
13. Richey, F.W.; McCloskey, B.D.; Luntz, A.C. Mg Anode Corrosion in Aqueous Electrolytes and Implications for Mg–Air Batteries. *J. Electrochem. Soc.* **2016**, *163*, A958–A963. [[CrossRef](#)]
14. Crowe, A.J.; Bartlett, B.M. Solid state cathode materials for secondary magnesium-ion batteries that are compatible with magnesium metal anodes in water-free electrolyte. *J. Solid State Chem.* **2016**, *242*, 102–106. [[CrossRef](#)]
15. Lam, R.; Marx, D.R. Ultra High Purity Magnesium Vacuum Distillation Ultra High Purity Magnesium Vacuum Distillation Purification Method. U.S. Patent 5,582,630, 1996.
16. Tayama, K.; Kimura, S. High Purity Metals, Process and Apparatus for Producing Them by Enhanced Purification. EP 1,335,030 A1, 2003.
17. Liu, M.; Uggowitz, P.J.; Nagasekhar, A.V.; Schmutz, P.; Easton, M.A.; Song, G.; Atrens, A. Calculated phase diagrams and the corrosion of die-cast Mg–Al alloys. *Corros. Sci.* **2009**, *51*, 602–619. [[CrossRef](#)]
18. Narayanan, T.S.N.S.; Park, I.; Lee, M. (Eds.) *Surface Modification of Magnesium and Its Alloys for Biomedical Applications: Mechanical Integrity of Magnesium Alloys for Biomedical Applications*; Elsevier: New York, NY, USA, 2015.
19. Xin, Y.; Huo, K.; Tao, H.; Tang, G.; Chu, P.K. Influence of aggressive ions on the degradation behavior of biomedical magnesium alloy in physiological environment. *Acta Biomater.* **2008**, *4*, 2008–2015. [[CrossRef](#)]

20. Hofstetter, J.; Martinelli, E.; Pogatscher, S.; Schmutz, P.; Povoden-Karadeniz, E.; Weinberg, A.; Uggowitz, P.; Löffler, J. Influence of trace impurities on the in vitro and in vivo degradation of biodegradable Mg–5Zn–0.3 Ca alloys. *Acta Biomater.* **2015**, *23*, 347–353. [[CrossRef](#)]
21. Cipriano, A.F.; Sallee, A.; Guan, R.-G.; Zhao, Z.Y.; Tayoba, M.; Sanchez, J.; Liu, H. Investigation of magnesium-zinc-calcium alloys and bone marrow derived mesenchymal stem cell response in direct culture. *Acta Biomater.* **2015**, *12*, 298–321. [[CrossRef](#)] [[PubMed](#)]
22. Höche, D.; Lamaka, S.V.; Vaghefinazari, B.; Braun, T.; Petrauskas, R.P.; Fichtner, M.; Zheludkevich, M.L. Performance boost for primary magnesium cells using iron complexing agents as electrolyte additives. *Sci. Rep.* **2018**, *8*, 7578. [[CrossRef](#)] [[PubMed](#)]
23. Wang, Y.C.; Tian, Y.; Qu, T.; Yang, B.; Dai, Y.; Sun, Y. Purification of Magnesium by Vacuum Distillation and its Analysis. *MSF* **2014**, *788*, 52–57. [[CrossRef](#)]
24. Bauer, R. Vakuumdestillation von Magnesium aus Aluminium-Magnesium-Legierungen und Aluminium-Magnesium-Silizium-Legierungen. Ph.D. Thesis, RWTH Aachen, Aachen, Germany, 1970.
25. Samanidis, K. Untersuchung der Destillation von Metallen im Vakuum. Ph.D. Thesis, RWTH Aachen, Aachen, Germany, 1989.
26. Zhu, T.; Li, N.; Mei, X.; Yu, A.; Shang, S. Innovative Vacuum Distillation for Magnesium Recycling. *Magnesium Technol.* **2001**, 55–60. [[CrossRef](#)]
27. Akbari, S.F. Minimizing Salt and Metal Losses in Mg-Recycling through Salt Optimization and Black Dross Distillation. Ph.D. Thesis, RWTH Aachen, Aachen, Germany, 2011.
28. Yong, D.; Bin, Y. *Vacuum Metallurgy of Nonferrous Metal Materials*; Metallurgical Industry Press: Beijing, China, 2000.
29. Liu, D.C.; Yang, B.; Wang, F.; Yu, Q.C.; Wang, L.; Dai, Y.N. Research on the Removal of Impurities from Crude Nickel by Vacuum Distillation. *Phys. Procedia* **2012**, *32*, 363–371. [[CrossRef](#)]
30. Kong, X.; Yang, B.; Xiong, H.; Liu, D.; Xu, B. Removal of impurities from crude lead with high impurities by vacuum distillation and its analysis. *Vacuum* **2014**, *105*, 17–20. [[CrossRef](#)]
31. Tao, D.P. A new model of thermodynamics of liquid mixtures and its application to liquid alloys. *Thermochimica Acta* **2000**, *363*, 105–113. [[CrossRef](#)]
32. Kong, L.; Yang, B.; Xu, B.; Li, Y.; Liu, D.; Dai, Y. Application of MIVM for Pb–Sn–Sb ternary system in vacuum distillation. *Vacuum* **2014**, *101*, 324–327. [[CrossRef](#)]
33. Yang, H.; Yang, B.; Xu, B.; Liu, D.; Tao, D. Application of molecular interaction volume model in vacuum distillation of Pb-based alloys. *Vacuum* **2012**, *86*, 1296–1299. [[CrossRef](#)]
34. Wang, A.; Li, Y.; Yang, B.; Kong, L.; Liu, D. Process optimization for vacuum distillation of Sn–Sb alloy by response surface methodology. *Vacuum* **2014**, *109*, 127–134. [[CrossRef](#)]
35. Revel, G.; Pastol, J.-L.; Rouchaud, J.-C.; Fromageau, R. Purification of Magnesium by Vacuum Distillation. *MTB* **1978**, *9*, 665–672. [[CrossRef](#)]
36. Löffler, J.; Uggowitz, P.; Wegmann, C.; Becker, M.; Feichtinger, H. Process and Apparatus for Vacuum Distillation of High-Purity Magnesium. WO 2013107644 A1, 2013.

